# Investigation of Electrical Performance of $HfO_2$-ZnO Bilayer Channels of Thin-Film Transistors using TCAD

Shashi Kant Dargar
Sir Padampat Singhania University
India

J. K. Srivastava
Sir Padampat Singhania University
India

Santosh Kumar Bharti
Sir Padampat Singhania University
India

## ABSTRACT

This paper shows the investigation of electrical performance of ZnO-based thin-film transistors (TFTs) with a multichannel layer. The multichannel TFTs consisting of $HfO_2$ and ZnO layers were deployed to insight of sufficient channel mobility and electrical stability. The obtained sub-threshold slope (1.69 ± 0.16 Volt/decade) decreased in comparison to single channel, with an increase in ON/OFF ratio $I_{ON}/I_{OFF}$ ($3.1 \pm 1.6 \times 10^5$). The device mobility is found increased due to addition the channel layer. The mobility achieved is $2.36 \times 10^{-3}$ $cm^2/V\text{-}s$. Due to the reduced interface trap density between the channel and dielectric layers, increases in the offset and the bandgap and improves the dielectric and interface quality. The oxide TFTs with a multilayer channel displayed comparatively good stability and mobility.

## Keywords

Hafnium-oxide ($HfO_2$), multilayer channel, thin-film transistor (TFT), ZnO , TCAD.

## 1. INTRODUCTION

Zinc oxide semiconductors that have been developed for the extensive controllability of their electrical and optical properties and their high transparency and mobility for optoelectronics applications [1]–[3]. Much effort has been particularly devoted to the development of ZnO-based oxide thin-film transistors (TFTs) for next-generation displays, such as large-scale active matrix organic light-emitting diodes, ultrafine-definition displays, transparent and flexible displays, and 3-D displays, because of their excellent high mobility, scalability, and low temperature processes [4]–[6]. Although oxide TFTs have shown adequate charge mobility for display operation, their instability under gate bias and illumination stress is currently one of the most critical issues that must be solved. The origin of the instability of oxide TFTs was attributed to the threshold voltage ($V_{th}$) being changed by the charge trapping and de-trapping in the gate-interface (gate insulator/channel layer), photo-generated carriers, and the back channel effect (molecular adsorption/desorption in the back channel) [7]–[9]. To obtain highly stable ZnO-based oxide TFTs, many studies have been devoted to the development of robust active layers by the incorporation of metal cations, such as Ga, Al, Hf, and Si [10]–[13], which are expected to reduce the density of defects, such as oxygen vacancies. However, these TFTs normally suffer from relatively low mobility. Thus, the fabrication of TFTs with high mobility and electrical stability is necessary for the application of next-generation displays. Several groups have suggested oxide TFTs with developed channels consisting of a buried layer and a bichannel layer deposited by sputtering, and high-stability TFT devices with appropriate mobility were reported [14]–[16]. Oxide-TFT devices can be applied to optical sensors for the remote control of touch screens. Fast-recovery and high-stability devices can be achieved using oxide TFTs with a multilayer channel [17].

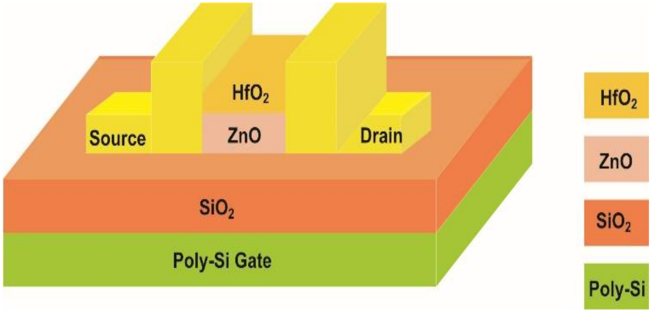


**Fig. 1. Schematic illustration of the TFTs with multilayer channel structure**

To analyze the origin of changes in the stability of the TFT devices, oxide TFTs with bottom gate structures is simulated using Sentaurus TCAD, as shown in Fig. 1. Finally, a novel oxide TFT with multichannel layers was designed by considering channel mobility and electrical stability.

## 2. PARAMETER EXTRACTION

The uniqueness of the thin film transistor technology lies in the composing materials and structure with few parameters on the substrate material and size. $V_{th}$ measured in volts, $I_{on/off}$, field effect mobility in $cm^2/Vs$ and sub threshold voltage in Volt/decade are the parameters which conclude the electrical performance of the device.

### 2.1 Threshold Voltage

The necessary gate voltage to turn the transistor ON is known as the threshold voltage. It should be low so that it takes low voltage to turn TFT on or off. It is measured in the saturation region i.e. $V_{DS} \geq V_{GS} - V_T$. Ids using square law model of TFT can be given by [12],[13] as indicated below in equation (1).

$$I_{ds}=\frac{1}{2}\mu C_G\left(\frac{W}{L}\right)\left(V_{GS}-V_{th}\right)^2 \quad (1)$$

where W, L, $C_G$ and μ are the TFT channel width, length, gate capacitance and field-effect mobility respectively. Measuring $V_{th}$ after square root the equation (1) we get (2)

$$\sqrt{I_{ds}} = \left\{\frac{1}{2}\mu C_G\left(\frac{W}{L}\right)\right\}^{\frac{1}{2}}(V_{GS} - V_{th}) \quad (2)$$

By plotting $\sqrt{I_d}$ *vs.* $V_{GS}$ and by extrapolating down to the x-axis, the threshold voltage can be determined.

### 2.2 Current On-Off ratio

Drain current on/off ratio is another measure of the switching behavior of the TFT. It is simply the ratio between highest measured current (the on-state current, $I_{on}$) to the lowest measured current (the off-state current, $I_{off}$). $I_{off}$ is also a measure of the gate leakage present in the device.

## 2.3 Field Effect Mobility

The mobility symbolizes rapid movement of an electron through a metal or a semiconductor in an applied electric field. Mobility is a proportionality constant which relates the drift velocity to the applied electric field. To estimate the carrier mobility the two commonly used definitions are effective mobility and field-effect mobility, extracted from the drain conductance $dI_d/dV_{DS}$ in linear regime and trans conductance $dI_{ds}/dV_{DS}$ $g_m$ of transfer characteristics, respectively. Field effect mobility is used as the estimator of TFT channel mobility.

## 2.4 Subthreshold Swing

Another important parameter is subthreshold slope, which describes the efficacy of the gate voltage in reducing drain current to zero, which is given by given by (3)

$$S = \frac{dV_{GS}}{d\log I_{ds}} \qquad (3)$$

To achieve high on/off current ratios, subthreshold slopes should be low so that the same difference in $V_{GS}$ can decrease the drain current by more decades. Above-threshold, subthreshold, and Poole-Frenkel emission are three regions achievable at different gate-source voltage. The region, where the TFT switches from off to on with exponential change in current from a low off current, which is in pA, to a high on current, which is in µA is recognized as subthreshold region. Forward subthreshold region is ranged with in $V_{TH} > V_{gs} > 0$. The drain current equation (4) in the forward subthreshold region is given by [14]

$$I_{DS} = \frac{I_{sub\,0}W}{L}\exp\frac{V_{GS}-V_{TS}}{S_f} \qquad (4)$$

where $I_{sub0}$ is the magnitude of current in the subthreshold region, and $S_f$ is the forward subthreshold region. The drain current equation (5) in the reverse subthreshold region is given as below.

$$I_{DS} = \frac{I_{sub\,0}W}{L}\exp\frac{V_{GS}-V_{TS}}{S_r+\gamma_n|V_{DS}|} \qquad (5)$$

where $S_r$ is the reverse subthreshold slope and $\gamma_n$ is a unitless parameter accounting for two dimensional effects.

## 3. SIMULATION

The simulation is performed using Sentaurus TCAD tool. The structure of multilayer thin film transistor is designed in the structure editor as shown in Fig. 2. The material has been chosen in the TFT as displayed in Schematic. The graphical User interface of Structure editor opens a window upon entering proper command line. This window has its three parts namely menu bar, toolbars, and the lists. Contacts can be defined to allow the constructed device to be connected to outside power sources. The contacts name, sets, properties, edge color, thickness are defined for the specific structure. Fig. 3 shows the designed structure of TFT with ZnO as an active channel layer in sentaurus structure editor.

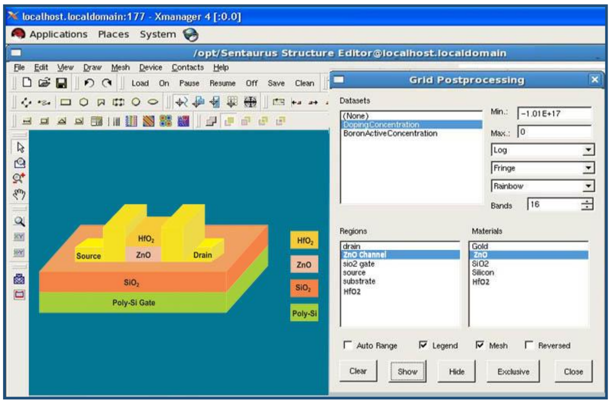


**Fig. 2. Design of TFT structure in the TCAD Structure Editor**

The doping profile has been set after the contact and edge setting. The layer of $HFO_2$ is chosen with different thickness to compare the performance in each case. Fig. 3 illustrates the doping profile and concentration gradient in multilayer structure. The variation in the oxide thickness has also been done to understand the effect of thickness in the mobility of the ZnO channel. The increase in the oxide thickness decreases the drain current at applied gate voltage as displayed in Fig. 4.

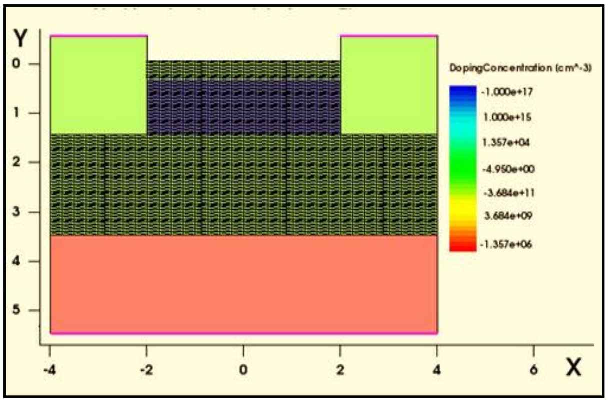


**Fig. 3. TFTs multilayer channel structure using 2D-Sentaurus Structure Editor**

It is noteworthy that because of the increased thickness the $V_{TH}$ parameter of the TFT, which is the necessary gate voltage to turn the transistor on, also increases.

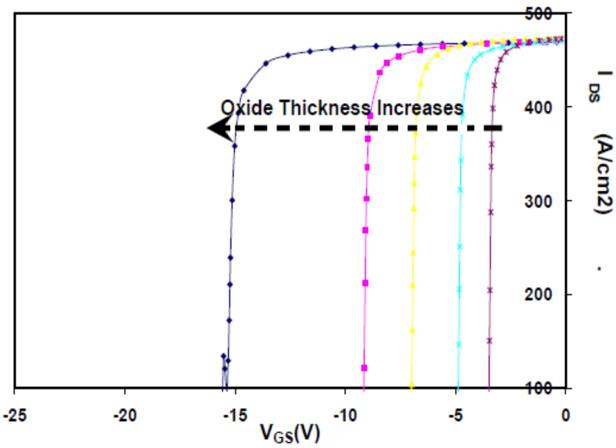


**Fig. 4. Effect of variation in oxide thickness**

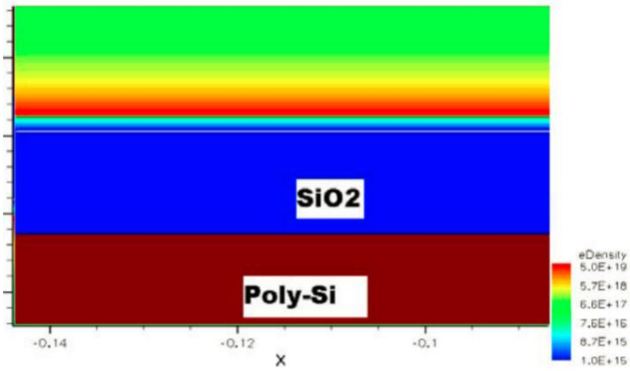


**Fig. 5. TFTs multilayer channel structure doping profile**

## 4. RESULT AND DISCUSSIONS

There is a good gate controllability in the ZnO TFTs. The single channel ZnO layer TFT is compared with the results from multilayer TFT. The TFT1, TFT2 and TFT3 multilayer with ZnO channel has $HfO_2$ thickness of 32-nm, 24-nm and 12-nm thickness respectively. Besides this, series of transistor parameters including subthreshold swing, $I_{ON/OFF}$ ratio, threshold voltage ($V_{th}$), and gate leakage current ($I_G$), were also calculated. The performance parameters, such as the threshold voltage ($V_{th}$), field-effect mobility ($\mu_{FE}$), Subthreshold swing, and variation of $V_{th}$ under gate bias are listed in Table I. However, our ZnO-TFTs showed a good mobility as compared to the results obtained by single channel ZnO TFT.

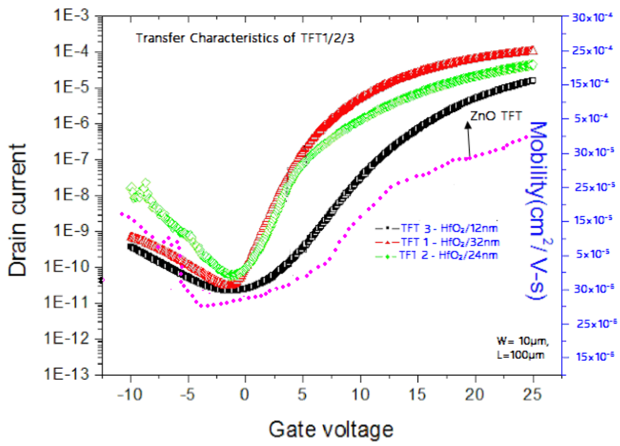


**Fig. 6. TFTs multilayer channel Transfer characteristics for TFT1/2/3.**

**Table 1. Summary of electrical performance of the oxide TFTs with various channel structures**

| Parameter | Multilayer channel Values | Single layer Channel ZnO Parameters |
|---|---|---|
| Threshold Voltage (V) | ~ 12 | 4.8 |
| ON current (A) | $0.66 \times 10^{6}$ | $5.22 \times 10^{-8}$ |
| Off current (A) | 0.21427 | $1.35 \times 10^{-11}$ |
| ON/OFF ratio | $3.1 \times 10^{5}$ | $3.86 \times 10^{3}$ |
| Mobility($cm^2$/V-s) | $2.36 \times 10^{-3}$ | $1 \times 10^{-4}$ |
| Sub-threshold slope(V/decade) | 1.69 ±0.16 | 1.94 |

From the simulation results that the gate-drain current voltage transfer characteristics are received as shown in Fig. 6. The results shows a wide increase in field effect mobility in the thicker $HfO_2$ layer.

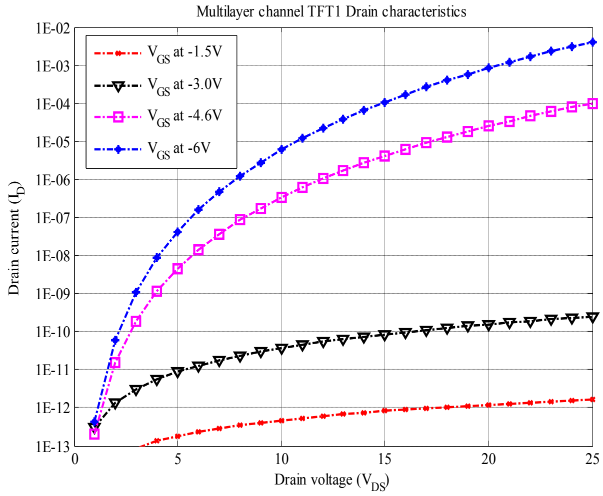


**Fig. 7. Drain Characteristics of the simulated multilayer TFT1 (32nm)**

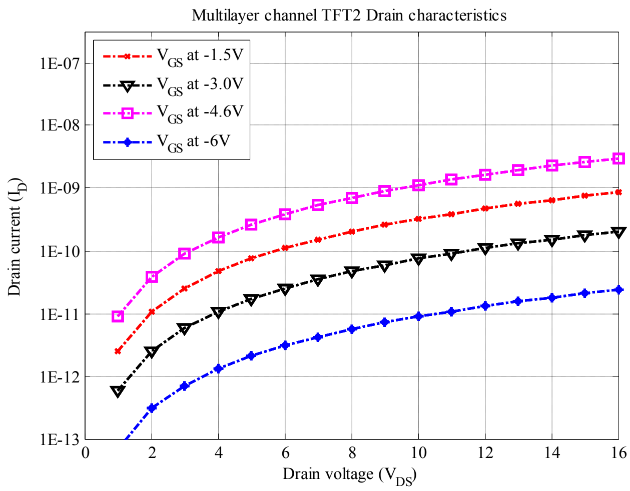


**Fig 8. Drain Characteristics of the simulated multilayer TFT2 (24-nm)**

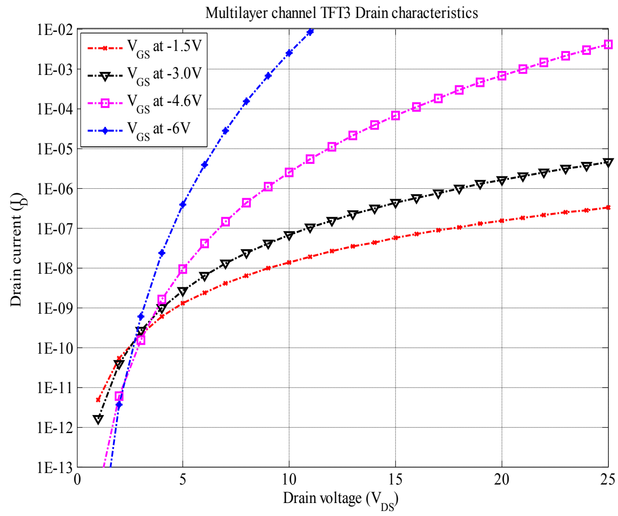


**Fig. 9 Drain Characteristics of the simulated multilayer TFT3 (12-nm)**

Fig. 7 and Fig. 8 shows the drain characteristics of the multichannel TFT1. The field-effect mobility *($\mu_{FE}$)* was determined by the maximum transconductance at a drain voltage ($V_D$) of 0.1 V. The subthreshold swing (SS) was extracted from the equation SS = ($dV_G/d$ log $I_{DS}$) at linear regions.

## 5. CONCLUSION

This has been observed that inclusion of hafnium affected the channel mobility, sub-threshold slope and bias stability in ZnO-based oxide TFTs. On the other hand, the oxide TFT with $HfO_2$ channel showed a significant improvement in stability, but resulted in poor mobility, owing to the reduction in channel electrical conductivity. The mobility of the oxide TFTs with the bi-channel layers found greater than that of the ZnO single layer TFT. The mobility of $2.36\times10^{-3}$ $cm^2$/V-s, hence, an increase in the $I_{ON}/I_{OFF}$ $3.1\times10^5$ has been obtained for the multichannel TFT, which is greater than that of the single layer ZnO TFT. Hence a channel structure with two layers is suggested. As a result of comparison, the multilayer oxide TFT displays relatively good channel mobility and bias stability to single and double-layer channels. Further, Oxide TFTs with proper stability and mobility can be produced with multichannel structures consisting of various oxide thin films with different thickness, electrical conductivity, and in accordance the application oriented composition may be used.

## 6. ACKNOWLEDGMENTS

Our sincere thanks to the experts and contributors of the authors of the journals whose original research work in this field laid the foundation of our work. We would like to extend our indebtedness to the affiliating university for the permissions and provisions of the simulations and availability of the tools in the laboratory.

## 7. REFERENCES

[1] Wager J. F. 2003 Transparent electronics, (May 2003) 1245-1246.

[2] Minami T., 2005 Transparent conducting oxide semiconductors for transparent electrodes, Semicond. Sci. Technol., (Mar. 2005) 535-544.

[3] Hoffman R. L., Norris B. H. and Wager J. F. 2003 ZnO-based transparent thin-film transistors, Appl. Phys. Lett. (Feb. 2003) 733-735.

[4] Nomura K., Ohta H., Takagi A., Kamiya T., Hirano M., and Hosono H., 2004 Room-temperature fabrication of transparent flexible thin-film transistors using amorphous oxide semiconductors Nature, (Nov. 2004) 488-492.

[5] Fortunato M. C., Barquinha P. M. C., Pimentel A. C. M. B. G., Goncalves A. M. F., Marques A. J. S., Pereira L. M. N., 2005 Fully transparent ZnO thin-film transistor produced at room temperature," Adv. Mater., (Mar. 2005) 590–594.

[6] Park S. K., Hwang C., Ryu M., Yang S., Byun C., Shin. J., 2005 Transparent and photo-stable ZnO thin-film transistors to drive an active matrix organic-light-emitting-diode display panel, Adv. Mater., (Mar. 2005) 590–594.

[7] Lopes M. E., Gomes H. L., Medeiros M. C. R., Barquinha P., Pereira L., Fortunato E., 2009 Gate-bias stress in amorphous oxide semiconductors thin-film transistors, Appl. Phys. Lett., (Aug. 2009) 063502-1-063502-3.

[8] Jeong J. K., Yang H. W., Jeong J. H., Mo Y.G., and Kim H. D., 2008 Origin of threshold voltage instability in indium-gallium-zinc oxide thin film transistors, Appl. Phys. Lett., (Sep. 2008) 123508-1–123508-3.

[9] Oh H., Yoon S. M., Ryu M. K., Hwang C. S., Yang S., and Park H. K., 2010 Photon-accelerated negative bias instability involving subgap states creation in amorphous In–Ga–Zn–O thin film transistor, Appl. Phys. Lett., (Nov. 2010) 183502-1–183502-3.

[10] Hosono H. 2006 Ionic amorphous oxide semiconductors: Material design, carrier transport, and device application, J. Non-Cryst. Solids, (Apr. 2006) 851–858.

[11] Ahn C. H., Kong B. H., Kim H., and Cho H. K., 2011 Improved electrical stability in the Al doped ZnO thin-film-transistors grown by atomic layer deposition, J. Electrochem. Soc., H170–H173.

[12] Kim C. J., Kim S., Lee H., Park J. S., Kim S., Park J., 2009 Amorphous hafnium-indium-zinc oxide semiconductor thin film transistors, Appl. Phys. Lett., (Dec. 2009) 252103-1–252103-3.

[13] Chong E., Jo K. C., and Lee S. Y., 2010 High stability of amorphous hafnium-indium-zinc-oxide thin film transistor, Appl. Phys. Lett., (Apr. 2010) 152102-1–152102-3.

[14] Kim J. I., Ji K. H., Jung H. Y., Park S. Y., Choi R., Jang M., 2011 Improvement in both mobility and bias stability of ZnSnO transistors by inserting ultra-thin InSnO layer at the gate insulator/channel interface, Appl. Phys. Lett., (Sep. 2011) 122102-1–122102-3.

[15] Chong E. and Lee Y., 2012 Influence of a highly doped buried layer for HfInZnO thin-film transistors, Semi Cond. Sci. Technol., (Jan. 2012) 012001-1-012001-4.

[16] Park J. C., Kim S., Kim C., Song I., Park Y. 2010 Highly stable transparent amorphous oxide semiconductor thin-film transistors having double-stacked active layers, Adv. Mater., (Dec. 2010) 5512–5516.

[17] Jeon S., Ahn S., Song I., Kim C. J., Chung U., Lee E., 2012 Gated three-terminal device architecture to eliminate persistent photoconductivity in oxide semiconductor photosensor arrays, Nature Mater., 301-305.